

NUMERICAL SIMULATION OF UNSTEADY ROTOR WAKES

A. Baron
Associate Professor

M. Boffadossi
PhD Student

Politecnico di Milano
Dipartimento di Ingegneria Aerospaziale
Via C. Golgi, 40 - 20133 Milano - Italy

Summary

A non linear unsteady vortex lattice scheme is presented. It is capable to predict the instantaneous configuration of the wake and the distribution of the aerodynamic load on rotor blades, during impulsive starts or arbitrarily unsteady flight conditions.

Any number of independent blades, with general planform and twist distribution, moving with assigned pitch and flap angles can be treated.

Rankine vortices are used to discretize vorticity. Turbulent diffusion of their cores is modeled in order to cope with the rapid roll-up process of unsteady and closely interfering wakes, without any form of tuning of the numerical parameters.

The capabilities of the code are verified by comparing numerical predictions with available steady state experimental data. Also reported are some results related to realistic unsteady flight conditions.

List of symbols

AR	blade aspect-ratio, $(R-r_0)/C$	r	dimensionless radial coordinate, r/R
c	local blade chord	r_c	vortex core radius
C	mean blade chord	r_0	cut-out radius
CL	local section lift coefficient, $2L/\rho(\Omega r)^2 c$	R	blade tip radius
CT	rotor thrust coefficient, $T/\rho(\Omega R)^2 \pi R^2$	\mathbf{R}	absolute position vector
\mathbf{e}	unit vector in the Biot-Savart law (Fig.1)	\mathcal{R}	rotation tensor
K	constant in the vortex core turbulent diffusion model	\mathcal{S}	surface of the cross section of an elementary portion of shear layer; surface of the cross section of the vortex core
l	spanwise dimension of the elementary portion of shear layer	t	time
L	section aerodynamic lift force	t_c	characteristic time, $2\pi/\Omega$
m	number of vortex segments on the lifting surfaces	t	dimensionless time, t/t_c
M	number of vortex segments released into the wakes	T	rotor thrust
n	number of blades	\mathbf{V}	absolute velocity
\mathbf{n}	local unit vector normal to the blade surface	\mathbf{W}	absolute angular velocity
r	radial coordinate	α	angle of attack of the rotor disk plane (positive for forward tilt)
		β	blade flap angle (positive upward)
		β_c	coning angle
		β_1	longitudinal flap angle

β_2	lateral flap angle	β_2	lateral pitch angle
ϕ	velocity potential	ψ	rotor blade azimuth angle;
γ	linear vortex density vector		dimensionless time, Ωt
Γ	bound circulation;	Ω	rotor rotational speed
	vortex strength		
μ	doublet strength;		Subscripts and superscripts:
	advance ratio, $V \cos \alpha / \Omega R$	B	blade
ρ	air density	H	rotor hub
σ	rotor solidity (ratio of blades area to rotor disk area)	k	index of the generic blade
θ	pitch angle (positive nose upward)	o	initial state
θ_c	collective pitch angle	SB	body surface
θ_1	longitudinal pitch angle	SW	wake surface

1 - Introduction

Helicopter rotors are characterized by high aspect-ratio blades trailing vorticity into the wake. This vorticity is mainly concentrated in the tip vortices. In hover, the axial convection of vorticity is produced only by the self-induced velocities of the wakes. In forward flight, the helical tip vortices are still subject to mutual induction, but are also convected rearward, as well as downward. So the wake consists of concentrated tip vortices trailed in skewed interlocking and distorting helices (Landgrebe and Cheney, 1972).

The strong interaction of tip vortices, either mutual or with lifting or solid surfaces, produces highly non linear phenomena which play a dominant role in the aerodynamic design of rotorcrafts. Accurate predictions of performances, vibrations, aeroelastic behaviour and noise generated by rotor blades are therefore strictly related to the ability to predict the instantaneous strength, structure and location of the shed wakes.

Unfortunately, a detailed solution of the time dependent fluid dynamic equations (Navier-Stokes equations) requires storage capabilities and computing times which still are unacceptable, even for a constant property fluid. However, when high Reynolds numbers are involved and flow separation is induced by sharp edges, Prandtl's hypotheses apply and simplified fluid dynamic equations can be used.

While retaining three dimensionality and unsteadiness, the flowfield can be assumed to be irrotational (being vorticity only confined in shear layers of negligible thickness) and therefore governed by a linear Laplace equation for the velocity potential.

Based on Prandtl's physical assumptions, a variety of mathematical formulations for the velocity potential has been developed in the past years (Hess and Smith, 1967; Morino and Kuo, 1974; Belotzerkowskii, 1977; Hunt, 1980; Katz and Maskew, 1988). An additional advantage of potential formulations, lies in the use of Green's theorem. This results in an integral equation the solution of which is required on the body's boundary only, rather than over a complex grid spanning the whole fluid volume.

Once the continuous vorticity distribution is discretized into vortex panels or filaments (vortex lattice schemes), the Biot-Savart law can be used to determine the velocity induced by the assigned distribution of vortices. As previously mentioned, at this stage, the flowfield of an incompressible fluid can be easily determined by solving a boundary integral form of a Laplace equation.

In principle, this can be done in a single step, provided the configuration of the vorticity containing sheets is assigned. As a matter of fact, this means that a correct knowledge of the flowfield must be known in advance.

In practice, it turns out that only for a limited number of relatively simple blade geometries and uniform flow conditions, such as hovering and vertical steady climb (for

which exhaustive experimental or empirical information is available), the geometry of the wakes can be assigned in a realistic way through the use of rigid or undisturbed wake models (Kocurek and Tangler, 1977).

Whenever an "a priori" estimate of the geometry of the wake becomes uncertain, e.g. because of the use of innovative blade planforms, numerical schemes based on rigid wake models necessarily fail. Free wake models (which rely on a first guess and successive corrections of the configuration of the wake, based on iterative solutions of the Laplace's equation) attempt to overcome these limitations by directly calculating the actual geometry of the wakes. Satisfactory results in the prediction of the performances of helicopter rotors in uniform flow can still be obtained (Summa and Maskew, 1981; Rosen and Graber, 1988; Felker et al., 1990).

However, when ground effects have to be accounted for, or when the rotor flow conditions are non uniform, either being unsteady the flight regime (e.g. take-off and landing, unsteady vertical climb, autorotation) or being unsteady the flow conditions encountered by each single blade (e.g. forward flight), the above mentioned techniques are no more applicable: unsteady schemes, capable to cope with the actual time dependent boundary and local flow conditions, and with the simultaneous presence of both tangential and radial time dependent components of the vorticity vector, must then be used (Ward, 1972; Johnson, 1990).

In the present work, a time marching scheme is proposed in which, starting from an initial state of rest, wakes and flowfield are computed simultaneously. Rotors are impulsively started and wakes are generated with a Lagrangian process during which, at each time step, the vorticity present on the edges of the blades is convected into the field.

With a time dependent approach, aerodynamic loads and geometry of the wakes during unsteady maneuvers can be easily simulated by considering the actual time dependent boundary conditions. These, including the effects of ground proximity, blade rotation, flap and pitch angles, define the instantaneous local velocity and the flight attitude of each blade element.

The present code, various applications of which are reported in section 5, is therefore capable to simulate general unsteady operation of helicopter rotors.

2 - The computational method

On the basis of a nonlinear vortex lattice scheme (Baron and Boffadossi, 1989; Baron et al., 1990) developed to model the unsteady incompressible flow past wings of arbitrary planform, a code for the prediction of wake configuration and load distribution on rotorcraft blades is derived.

The basic assumptions, relationships and limitations of the method are briefly summarized in the following.

The blades are assumed to have a negligible thickness and are simulated as rigid, plane or cambered surfaces with arbitrary twist and taper distribution.

They can undergo a general unsteady motion, including flapping and pitching effects.

Geometry of the wakes and distribution of aerodynamic loads are predicted, as a function of time, starting from an initial state of rest.

Wakes can be released in the flowfield from any of the sharp edges of the blades, depending on planform, aspect ratio and attitude of the blades.

The code can treat general rotor configurations and blade planforms, provided that lines along which wake separation takes place (regardless of their number and location) are assigned a priori.

The unsteady flow of an incompressible ideal fluid is irrotational in the region outside the lifting surfaces and the separated vortex sheets. It is therefore governed by Laplace's equation:

$$\nabla^2 \phi(\mathbf{R}, t) = 0 \quad (2.1)$$

where ϕ is the velocity potential at time t , expressed in terms of the absolute position vector \mathbf{R} .

The second order, linear differential equation (2.1) can be solved once appropriate boundary conditions are prescribed at any time t . These satisfy the far field condition ($\nabla\phi=0, \mathbf{R}=\infty$) and the no-penetration condition on the material surfaces SB:

$$[\nabla\phi(\mathbf{R}, t) - \mathbf{V}^B(\mathbf{R}, t)] \cdot \mathbf{n}(\mathbf{R}, t) = 0 \quad \text{on SB} \quad (2.2)$$

where $\mathbf{V}^B(\mathbf{R}, t)$ is the local body velocity vector and $\mathbf{n}(\mathbf{R}, t)$ is the local unit vector normal to the surface.

In addition, when flight in ground effect has to be simulated, the no-penetration condition on the ground surface is satisfied using the virtual image technique.

Using Green's theorem according to Hunt (1980), the velocity at point P and time t , can be written in the usual integral form:

$$\begin{aligned} \mathbf{V}_P = \nabla_P \phi = \frac{1}{4\pi} \iint_{SB} \Delta\phi_Q \nabla_P \left[\nabla_Q \left(\frac{1}{|\mathbf{P}-\mathbf{Q}|} \right) \cdot \mathbf{n}_Q \right] dS_Q + \\ + \frac{1}{4\pi} \iint_{sw} \Delta\phi_Q \nabla_P \left[\nabla_Q \left(\frac{1}{|\mathbf{P}-\mathbf{Q}|} \right) \cdot \mathbf{n}_Q \right] dS_Q \end{aligned} \quad (2.3)$$

where ∇_P and ∇_Q denote the gradient operators evaluated in P and Q, $|\mathbf{P}-\mathbf{Q}|$ is the distance between point P and the generic point Q laying on the lifting surfaces SB or on the vortex sheets sw across which the jump in the velocity potential ϕ is $\Delta\phi_Q$.

For the solution of equation (2.3) wings and wakes are discretized into a finite number of surface panels with constant doublet strength $\mu = \Delta\phi$. Due to the equivalence between doublet and vorticity distributions (Hoeijmakers, 1989), each panel is therefore made up of straight vortex segments lying on its perimeter, forming a closed loop of circulation $\Gamma = \Delta\phi$ (Mook, 1988).

Note that closed loop vortices are more convenient than usual horseshoe vortices for representing both the tangential and radial vorticity components present in time dependent flows.

Once vorticity has been discretized and Biot-Savart law is applied, equation (2.3) reduces to:

$$\begin{aligned} \mathbf{V}(\mathbf{R}, t) = \mathbf{V}^{SB}(\mathbf{R}, t) + \mathbf{V}^{sw}(\mathbf{R}, t) = \\ \frac{1}{4\pi} \sum_{i=1}^m \left[\frac{\cos\vartheta_A(\mathbf{R}, t) - \cos\vartheta_B(\mathbf{R}, t)}{h(\mathbf{R}, t)} \Gamma(t) \right] \mathbf{e}_i(\mathbf{R}, t) + \\ + \frac{1}{4\pi} \sum_{j=1}^{M(t)} \left[\frac{\cos\vartheta_A(\mathbf{R}, t) - \cos\vartheta_B(\mathbf{R}, t)}{h(\mathbf{R}, t)} \Gamma(t) \right] \mathbf{e}_j(\mathbf{R}, t) \end{aligned} \quad (2.4)$$

where m and M are the number of vortex segments laying on the lifting surfaces and on the

free wakes respectively. The terms in equation (2.4) are identified in Fig.1.

Note that when the velocity is computed at a point laying on a lifting surface, one has to account for the self-induced tangential velocity due to the local strength of the vortex sheet.

The unknown values of the N circulations $\Gamma(t)_i$ on the lifting surface panels are determined, at each time step, imposing the zero normal velocity condition (2.2) on the panel control points. Velocities are evaluated at control points through equation (2.4). The following linear system of N algebraic equations must then be solved at each time t :

$$\sum_{i=1}^N A(t)_{ij} \Gamma(t)_j = \left[\mathbf{V}^B(t) \cdot \mathbf{n}(t) \right]_i - \left[\mathbf{V}^{SW}(t-\Delta t) \cdot \mathbf{n}(t) \right]_i \quad (i=1,N) \quad (2.5)$$

where:

$A(t)_{ij} = (\mathbf{V}^{SB} \cdot \mathbf{n})_i$ is the normal component of the velocity induced, at time t , in the control point of the i -th panel by a unit circulation lying on the j -th panel;

$\Gamma(t)_j$ is the circulation on the j -th panel, at time t ;

$\mathbf{V}^B(t)_i$ is the velocity of the control point of the i -th panel ensuing from the unsteady motion of the lifting surface;

$\mathbf{V}^{SW}(t-\Delta t)_i$ is the velocity induced by the wakes on the control point of the i -th panel at time $(t-\Delta t)$, which, at time $t=0$, is assumed equal to zero, consistently with the hypothesis of impulsive start;

$\mathbf{n}(t)_i$ is the unit vector normal to the i -th panel, at time t .

Starting from rest, wakes are generated in a Lagrangian process, by releasing in the field the vorticity present on the edge panels. At the instant motion begins no vorticity has been convected, so no wakes exist but a starting vortex forms along the sharp edges and is subsequently shed into the field.

In order to obtain this, panels from the edges along which vorticity is shed are "moved" into the field and form a first row of wake panels. At the following time steps, each node of the existing wake is convected to a new position and a new row of panels is added to the wakes.

The instantaneous local velocity is computed and used to displace the nodes in order to produce force free vortical sheets.

Displacement of the wake nodes is obtained by integrating the velocity according to the second order Adams-Bashforth formula:

$$\mathbf{R}(t+\Delta t) = \mathbf{R}(t) + \left[\frac{3}{2} \mathbf{V}(t) - \frac{1}{2} \mathbf{V}(t-\Delta t) \right] \Delta t \quad (2.6)$$

According to Kelvin's theorem, vorticity is conserved and circulation around each vortex segment in the wakes remains constant.

The distribution of the net pressure coefficient on the lifting surfaces is calculated by using Bernoulli's unsteady equation, written in a blade fixed frame of reference (Kandil, 1985). Total load coefficients are obtained by integration of pressure distributions.

3 - Definition of the frames of reference

For the solution of equation (2.5) appropriate coordinate systems must be selected in order to express the instantaneous location, attitude and velocity of each blade element in the absolute frame of reference.

Coefficients of the aerodynamic influence matrix $[A(t)]$ depend in fact on geometry and position of the rotor blade elements (both mutual and with respect to the ground). Moreover, the velocity of the control point of each blade panel must be prescribed. This is the result of flapping and rotation of the blades, and of both linear and angular velocities of the rotorcraft. Offset of the hinges and lag motion of the blades are not considered in the present work.

At time t , the absolute position vector $RP(t)$ of a generic point P, laying on the k -th blade, can be expressed as a function of its initial position P_0 :

$$RP(t) = \mathcal{R}(t) \mathcal{R}_k(t) RP_0 + RH(t) \quad (3.1)$$

where $RP_0 = P_0 - H_0$, $RH(t) = H(t) - H_0$, $H(t)$ denotes the position of the rotor hub at time t , and H_0 its location at time $t=0$.

$\mathcal{R}(t)$ is the tensor associated with the rotation of the helicopter with respect to its orientation in the initial state of rest ($t=0$). $\mathcal{R}_k(t)$ is the tensor associated with the rotation of the k -th blade, with respect to initial values of azimuthal, flapping and pitching angles. $\mathcal{R}_k(t)$ therefore includes the contributions of instantaneous azimuthal angle $\psi_k(t)$, flapping angle $\beta_k(t)$ and pitching angle $\vartheta_k(t)$, for the k -th blade, defined by:

$$\psi(t)_k = \Omega t + 2\pi(k-1) / n \quad (3.2)$$

$$\beta(t)_k = \beta_c(t) - \beta_1(t) \cos\psi(t)_k - \beta_2(t) \sin\psi(t)_k \quad (3.3)$$

$$\vartheta(t)_k = \vartheta_c(t) - \vartheta_1(t) \cos\psi(t)_k - \vartheta_2(t) \sin\psi(t)_k \quad (3.4)$$

Therefore, at time t , the absolute velocity of a generic point P laying on the k -th blade can be determined according to:

$$VP(t) = W_k(t) \wedge (RP(t) - RH) + V_H \quad (3.5)$$

where $W_k(t)$ is the instantaneous angular velocity of the k -th blade, consequent to maneuvering angular velocity of the helicopter, rotational speed of the rotor, and blade flapping and pitching motions.

4 - Vortex core and turbulent diffusion modeling

The assumptions made in sections 1 and 2 lead to concluding that the velocity, at any generic point in the flowfield, can be determined as a function of the instantaneous distribution of vorticity bound to the lifting surfaces and convected into the free shear layers.

Both bound and free vorticity are distributed in space in a continuous way. However, for the numerical solution of the flowfield, wakes and lifting surfaces must be discretized into a finite number of vorticity containing panels or, equivalently, in a lattice of vortex filaments.

Vortex filaments are extremely efficient from a computational point of view and their use is in practice compulsory when iterative or time marching schemes have to be used. Nevertheless, they introduce in the flowfield lines along which, according to the Biot-Savart law, induced velocity tends to infinity.

This situation is not only unrealistic from a physical point of view, but can also turn out

to be numerically inadequate to simulate flows in which regions of high vorticity are present (typically the roll-up region of closely interfering blade tip vortices). The singular behaviour of vortex filaments can be such to produce numerical instabilities and may cause the solution to diverge (Baron and Boffadossi, 1989).

This problem can be eliminated by preventing the induced velocity, at points close to the vortex axes, from increasing above a certain value. This can be done in a variety of ways and basically consists in introducing what is called a vortex, or vortex core, model.

In the past, various attempts were done to adopt a cut-off radius below which the velocity induced by vortex filaments was assumed to be equal to zero (Mook, 1988). Rankine vortices, which approximate to a larger extent the physical behaviour of real vortices (Rusak et al., 1985; Buresti et al., 1989; Baron and Boffadossi, 1989) and various artificial diffusion laws for the vortex cores (Bloom and Jen, 1974) have also been used.

However, induced velocities, and related solutions, depend significantly on the numerical values assigned to the cut-off or viscous core radius, or to the empirical constants involved in the vortex core diffusion laws. As a consequence, a careful tuning of the vortex core models was required in order to deal with each particular application (i.e. wing or blade aspect ratio and planform, angle of attack, geometrical discretization, etc.).

Furthermore, most of the discrete vortex methods, and vortex lattice among them, are only consistent with the vorticity convection equation but completely neglect diffusion. Therefore, when diffusion becomes a prevailing phenomenon (i.e. in the roll-up region of the wake), it must be accounted for by an explicit model.

A physically consistent turbulent diffusion mechanism can therefore significantly extend the simulation capability of vortex lattice schemes.

In the present work, a diffusion mechanism for the vortex cores is adopted, recently formulated following the diffusion process of turbulent shear layers (Baron et al., 1990). While retaining the intrinsic simplicity of the Rankine vortex model, a diffusion law for its core radius has been derived, capable to overcome, in a general way and without any form of tuning, the above mentioned difficulties.

Vorticity shed in the rotor flowfield is mainly concentrated in the blade tip vortices, originated by the intense roll-up of the continuous wakes released at trailing edges. Accordingly, Rankine vortices are assumed to be "equivalent" to the elementary portions of the physically continuous shear layers they replace in the numerical scheme. Their core radii will therefore spread in such a way that their cross sectional area S and circulation $\Gamma = \gamma l$ are equal, at each time, to spreading and circulation of an elementary portion of continuous shear layer containing the same vorticity (Fig.2). This implies a rate of change of their radius r_c given by:

$$\frac{dr_c}{dt} = \frac{K \Gamma}{2 \pi r_c} \quad (4.1)$$

where the diffusion constant K , both for forced and unforced turbulent shear layers, assumes a universal value equal to 0.095, as demonstrated by experimental evidence (Liepmann and Laufer 1947; Brown and Roshko, 1974; Oster and Wygnanski, 1982; Lesieur, 1987).

This relation states that Rankine vortex core diffusion must be:

- proportional to the circulation Γ of the vortex,
- inversely proportional to its radius,
- independent on transversal stretching, namely on the rate of change of the distance between the axes of the vortices.

Equation (4.1) is then used to model the core diffusion process of each Rankine vortex in the vortex lattice scheme.

A final observation can be done on the vortex core diffusion model. As previously mentioned, other techniques turn out to be strongly dependent on the number of vortex filaments used to discretize the continuous distribution of vorticity in the flowfield (Rusak et al., 1985). The present approach, on the contrary, is virtually independent on discretization, the turbulent diffusion being explicitly related to the circulation of each vortex filament and, therefore, to the number of vortices. This brings to a kind of "self adaptation" of the model and explains why, in a variety of applications, no tuning has been required for a correct simulation of the vortex core diffusion.

5 - Numerical results

Some applications of the unsteady vortex lattice scheme are presented in the following. They aim to comparing numerical predictions of the present method to experimental data available in the literature (section 5.1), and to illustrating the capabilities of the code.

Although the present method can treat either impulsive starts or general unsteady motion of rotor blades, comparative experimental data are only available for the steady state condition. This implies that transient computations can only be discussed in qualitative terms.

Prior to proceeding further in the analysis of the numerical results, some general comments are made on the choice of the numerical parameters, spatial and time discretizations.

Turbulent diffusion of the cores of the discrete vortices is modelled according to equation (4.1), which involves neither a tuning nor a choice of numerical parameters. On the contrary, the use of a self-adapting law for the diffusion of vortex cores makes the numerical scheme quite insensitive to the geometrical discretization of the wakes.

Refinement of the geometrical discretization of the lifting surfaces obviously brings to an increasingly better definition of the load distribution on the rotor blades, but also requires rapidly growing computing times. For rotor blades having rectangular planform and relatively high aspect-ratio, a preliminary analysis of the sensitivity of the scheme to panel density has shown that an accurate prediction of the aerodynamic loads can be obtained even by using a limited number of vortex panels: typically 4 by 6 panels, in chordwise and spanwise directions. Solutions are only negligibly improved by further increase of the number of panels.

Flowfield and aerodynamic load on rotor blades rely upon the instantaneous location of the shed wakes, the time evolution of which is governed by equation (2.6). Therefore, an appropriate integration time step must be used to accurately evaluate the displacement of the nodes of the vortex lattice. Moreover, the time discretization also affects the longitudinal dimension of the vortex panels in the wake, so influencing the uniformity of the vortex elements. Though not strictly compulsory, time discretization should be such to produce nearly uniform vortex elements on wakes and lifting surfaces. These are known to increase accuracy of the solutions and stability of the numerical scheme.

All the numerical results presented in the following have been obtained using a dimensionless integration time step equivalent to 1/32 of rotor revolution. This value meets rather well the antithetical requirements of accuracy and computing time.

5.1 - Validation of the code: two-bladed rotor in hover O.G.E.

The numerical simulation of this flight condition is not critical. Nevertheless it can be used to validate the code, because of the exhaustive experimental data available for helicopter rotors in hover.

Here the well known experiments by Caradonna and Tung (1981), concerning a two-bladed rotor,

have been selected to check the accuracy of the numerical predictions. Blades are untwisted, have constant chord, their aspect-ratio is equal to 6 and the collective pitch angle is 8 degrees. In the numerical scheme blades have been discretized using 4 chordwise and 6 spanwise vortex panels.

The time dependent evolution of the rotor wake is displayed in Fig.3, at four stages of its development (1, 2, 4 and 10 rotor revolutions).

Note that the thickness of the solid lines, representing vortical filaments in the wake, is proportional to the circulation of each vortex filament. Only the wake of a single blade is shown for clarity.

An intense starting vortex forms in the initial stage of the impulsive start. Then vorticity is continuously released in the field from the trailing edge of the blade and tends to concentrate in the tip vortices. During the initial phase of the development of the wake, vorticity remains confined in the vicinity of the rotor disk, until an axial velocity field is produced by the self-inducing action of the wake. The vortex filaments are then convected downstream, the inducing effect of the starting vortices progressively vanishes and an almost steady state configuration of the near-wake is attained within four to five rotor revolutions. At this stage, the typical contraction of the wake becomes evident.

For the same rotor and flight condition, the time evolution of thrust coefficient C_T , consequent to an impulsive start, is reported in Fig.4.

Thrust rapidly increases in the initial stage of the impulsive start, until each blade (half rotor revolution after start) interacts with the starting vortex shed in the field by the preceding blade. At this point, close blade vortex interaction and simultaneous regular development of the self-induced velocity field cause the thrust coefficient to reduce and progressively tend toward a steady state value equal to 0.0046, which coincides exactly with the experimental result (Caradonna and Tung, 1981).

In spite of the relatively reduced number of panels, the radial distribution of lift coefficient (Fig.5) quite closely matches the steady state measurements.

5.2 - Two-bladed rotor in hover I.G.E.

Operations of helicopter rotors close to ground are an example of a relatively simple flight condition in which numerical techniques based on prescribed wake models prove to be useless and recourse to unsteady free wake models is a must. Such flight conditions require the simulation of wakes developing close and impinging on a solid surface, and imply a modeling of the interaction of vortex filaments with ground.

In the present work, the ground effect is simulated using the virtual image technique. Possible interactions between vortex filaments and ground are controlled by imposing a minimum distance of their axes from ground equal to the instantaneous radius of their viscous cores, computed according to equation 4.1.

Results are reported in Fig.6 and 7 for the previously described rotor of Caradonna and Tung (1981), at the same collective pitch angle of 8 degrees, impulsively started in ground effect. Two different values of the distance of the rotor plane from ground are examined, equal to 0.25 and 0.5 rotor tip radius R . Results concerning hover O.G.E are also reported for comparison.

In Fig 6 a plan view of the wakes is shown, after three rotor revolutions, for the different values of the distance of the rotor plane from ground. Again, only the wake of a single blade is shown and line thickness is proportional to vortex strength.

Ground proximity produces a significant radial spreading of the rotor wake. Radial spreading of the wake increases the distance between blades and tip vortices released in the flowfield. This reduces their downward inducing effect through the rotor disk.

Consequently, thrust produced by the rotor is increased when reducing its distance from ground.

This is clearly confirmed by both the time history and by the steady state values of the thrust coefficient (Fig.7). Note that thrust is only negligibly affected by ground proximity during the initial stage following the impulsive start. This is ascribable to the fact that the wakes, immediately after start, are still close to the rotor plane, and their distance from ground is such that no appreciable effect is induced on wakes and, therefore, blades. Only when self-induction progressively brings the wakes close to the ground (this happens as earlier as lower is their initial distance from ground), their evolution and rotor thrust are effectively modified.

Ground proximity induces a radial spreading of the outer part of the wake (tip vortices), however it confines the inner part of the wake between rotor disk plane and ground. This causes persistence of vortex filaments close to the rotor disk and induces oscillations in the time evolution of thrust. Such oscillations disappear only when the rotor distance from ground is relatively high.

5.3 - Two-bladed rotor in climbing forward flight

In steady climbing flight, unless vertical, blade motion must include flapping and pitching, and flow conditions encountered by each single blade are actually changing with time. The helical wakes released by the rotor blades are still subject to mutual induction, but are also convected rearward, as well as downward. Also this situation requires recourse to unsteady numerical schemes, capable to cope with time dependent local flow conditions.

The time evolution of wake and thrust coefficient C_T are presented, for a two-bladed rotor impulsively started in climbing forward flight with an advance ratio μ equal to 0.05, and an angle of attack α of the rotor disk plane equal to 45 degrees. Rotor blade characteristics are the following: tip radius $R=5.08\text{m}$, cut-out radius $r_o=1.016\text{m}$, constant chord $C=0.33\text{m}$, $AR=12.31$.

Approximate control laws for flapping and pitching motions (see equations 3.3 and 3.4) have been derived, and imposed to the motion of the blades, using a numerical method based on strip theory. The use of strip theory for this flight condition brings to local instantaneous flap and pitch angles:

$$\beta(t)_k = 1.5 - 0.82 \cos\psi(t)_k$$

$$\vartheta(t)_k = 9.46 - 1.86 \sin\psi(t)_k$$

The time evolution of the wake is shown in Fig.8. Again, only the wake of a single blade is drawn, after 1, 2, 3, 4 and 7 rotor revolutions, and line thickness is proportional to vortex strength.

The starting wake grows in a regular way and is then progressively convected as well as distorted by self-induction effects. Note that, once two rotor revolutions have completed, the configuration of the near-wake remains practically unchanged.

This is also confirmed by the time history of the thrust coefficient (Fig.9), which rapidly tends toward an oscillatory behavior with constant amplitude and frequency. The contribution to thrust of each single blade is also shown in Fig.9.

5.4 - Unsteady vertical take off I.G.E.

Finally, the vortex lattice scheme is applied to the simulation of an unsteady vertical take off in ground effect. In this flight condition, unsteadiness is due both to time dependent boundary conditions (rotor disk distance from ground changes with time) and to the

unsteady helicopter motion (the vertical velocity of which increases with time). Ground effect is simulated again by using the virtual image technique and interaction between vortex filaments and ground is controlled by imposing a minimum distance of their axes from ground equal to the instantaneous radius of their viscous cores.

Rotor blade characteristics are the same as those used in section 5.3. The rotor is impulsively started, its initial distance from ground is equal to $0.5 R$ (2.54 m), and blade collective pitch angle θ_c is equal to 12 degrees.

Thrust is computed at each time step and applied to the center of gravity of the rotor, where the entire mass of the helicopter (equal to 1500 Kg) is concentrated. Obviously, a more realistic simulation of helicopter maneuvers can be obtained, provided accurate dynamic models of both helicopter and rotor are adopted, along with appropriate control laws.

The time history of the helicopter vertical acceleration a_z and its distance from ground z are reported in Fig.10, while the time dependent development of the wake is shown in Fig.11.

6 - Conclusions

A vortex lattice scheme for the prediction of flowfield and load distribution on rotor blades in general unsteady motion has been developed. Various flight conditions, ranging from hover I.G.E to forward flight and unsteady take off have been simulated. Reasonable results have been obtained, without resorting to any form of tuning of the free wake.

The satisfactory behavior of the code, in such unsteady flow conditions as impulsive starts, is probably related to the use of a physically consistent model for the turbulent diffusion of the viscous cores of the discrete Rankine vortices. Although further investigations are required, this vortex core diffusion mechanism seems to be capable to cope with the crucial aspects of the interaction of vortical filaments with solid surfaces.

In the present work, no attempt has been carried out aimed at increasing the computational efficiency of the numerical scheme. Various techniques, based on approximate treatment of the far-wakes are envisaged, which will be the subject of future investigations.

Acknowledgments

This work has been partially supported during 1990 by the Ministero dell'Universita' e della Ricerca Scientifica e Tecnologica.

References

- BARON A., BOFFADOSSI M. (1989), "Simulazione numerica di scie vorticose non stazionarie tridimensionali", Proceedings of the X Convegno Nazionale di Aeronautica e Astronautica, Pisa.
- BARON A., BOFFADOSSI M., DE PONTE S. (1990), "Numerical simulation of vortex flows past impulsively started wings", AGARD-CP "Vortex Flow Aerodynamics", paper N.33.

- BURESTI G., LOMBARDI G., PETAGNA P. (1989), "Analisi dell'interazione fra superfici portanti mediante un modello potenziale", *Proceedings of the X Convegno Nazionale di Aeronautica e Astronautica*, Pisa.
- BELOTZERKOWSKII S.M. (1977), "A study of unsteady aerodynamics of lifting surfaces using the computer", *Ann.Rev.Fl.Mech.*, Vol.9, pp. 469-494.
- BLOOM A.M., JEN H. (1974), "Roll-up of aircraft trailing vortices using artificial viscosity", *J. of Aircraft*, Vol.11, No.11, pp. 714-716.
- BROWN G.L., ROSHKO A. (1974), "On density effects and large structure in turbulent mixing layers", *J.Fl.Mech.*, Vol.64, pp. 775-816.
- CARADONNA F.X., TUNG C. (1981), "Experimental and analytical studies of a model helicopter rotor in hover", *Vertica*, Vol.5, N.2, pp.149-161.
- FELKER F.F., QUACKENBUSH T.R., BLISS D.B., LIGHT J.S. (1990), "Comparison of predicted and measured rotor performance in hover using a new free wake analysis", *Vertica*, Vol.14, N.3, pp.361-383.
- HESS J.L., SMITH A.M.O. (1967), "Calculation of potential flow about arbitrary bodies", *"Progress in Aeron. Sciences"*, Vol.8, Pergamon Press, pp. 1-138.
- HOEIJMAKERS H.W.M. (1989), "Computational vortex flows aerodynamics", AGARD-CP 342.
- HUNT B. (1980), "The mathematical basis and numerical principles of the boundary integral method for incompressible potential flow over aerodynamic configuration", in *"Numerical Methods Applied in Fluid Dynamics"*, Ed. by B.Hunt, Academic Press, London, pp. 49-135.
- JOHNSON W. (1990), "Airloads and Wake Models for a Comprehensive Helicopter Analysis", *Vertica*, Vol.14, N.3, pp.255-300.
- KANDIL, O.A. (1985), "Steady and unsteady incompressible free-wake analysis", in *"Computational Methods in Potential Aerodynamics"*, Ed. by Morino, Springer-Verlag.
- KATZ J., MASKEW B. (1988), "Unsteady low speed aerodynamics model for complete aircraft configurations", *J. of Aircraft*, Vol.25, No.4, pp 302-310.
- KOCUREK J.D., TANGLER J.L. (1977), "Prescribed wake lifting surface hover performance analysis", *J. of the American Helicopter Society*, Vol.22, N.1, pp.24-35.
- LANDGREBE A.J., CHENEY M.C. (1972), "Rotor Wakes - Key to Performance Prediction", AGARD-CP-111.
- LESIEUR M. (1987), "Turbulence in fluids, stochastic and numerical modelling", Martinus Nijhoff Publishers, Dordrecht.
- LIEPMANN H.W., LAUFER J. (1947), "Investigation of free turbulent mixing", NACA-TN-1257.
- MOOK D.T. (1988), "Unsteady aerodynamics", VKI L.S. 1988-07 on "Unsteady Aerodynamics".
- MORINO L., KUO C.C. (1974), "Subsonic potential aerodynamics for complex configurations: a general theory", *AIAA J.*, Vol.12, No.2, pp. 191-197.
- OSTER D., WYGNANSKI I. (1982), "The forced mixing layer between parallel streams", *J.Fl. Mech.*, Vol.23, pp. 91-130.
- ROSEN A., GRABER A. (1988), "Free wake model of hovering rotors having straight or curved blades", *J.of the American Helicopter Society*, Vol.30, N.3, pp.11-19.
- RUSAK Z., SEGNER A., WASSERSTROM E. (1985), "Convergence characteristic of a vortex-lattice method for nonlinear configuration aerodynamics", *J. of Aircraft*, Vol.22, No.9, pp. 743-749.
- SUMMA J.M., MASKEW B. (1981), "A surface singularity method for rotors in hover or climb", USA AVRADCOM-TR-81-D23.
- WARD J.F. (1972), "A Summary of Current Research in Rotor Unsteady Aerodynamics With Emphasis on Work at Langley Research Center", AGARD-CP-111.

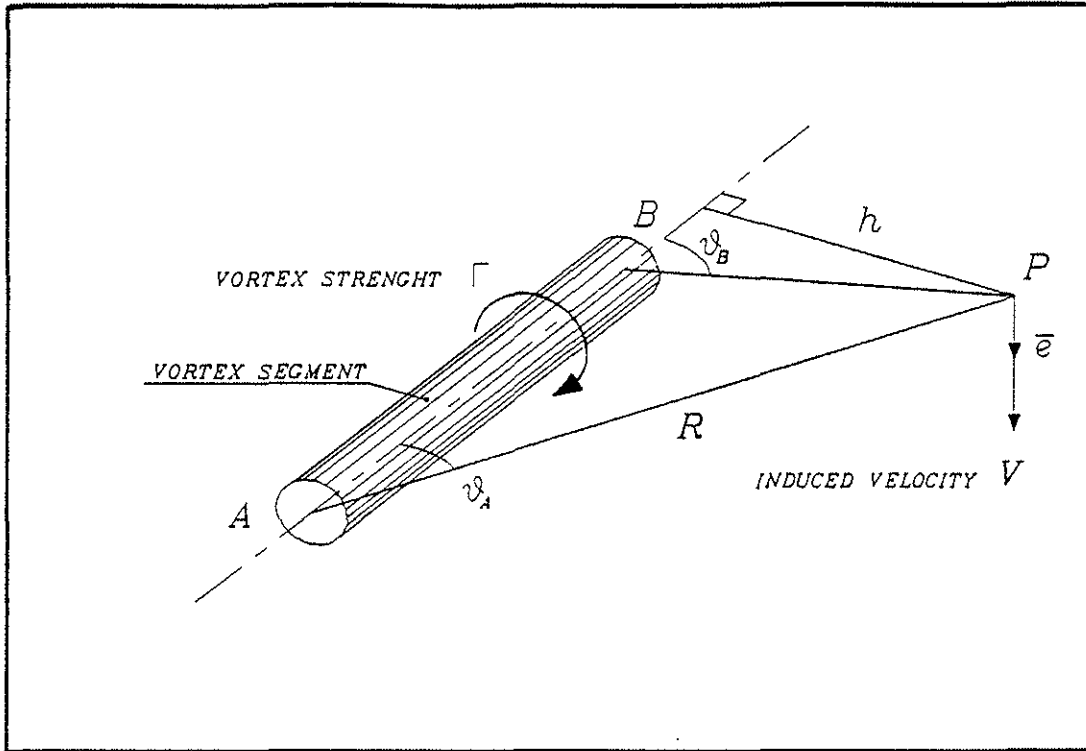


Fig.1 - Velocity induced by a vortex segment. Definition of the variables appearing in the Biot-Savart law.

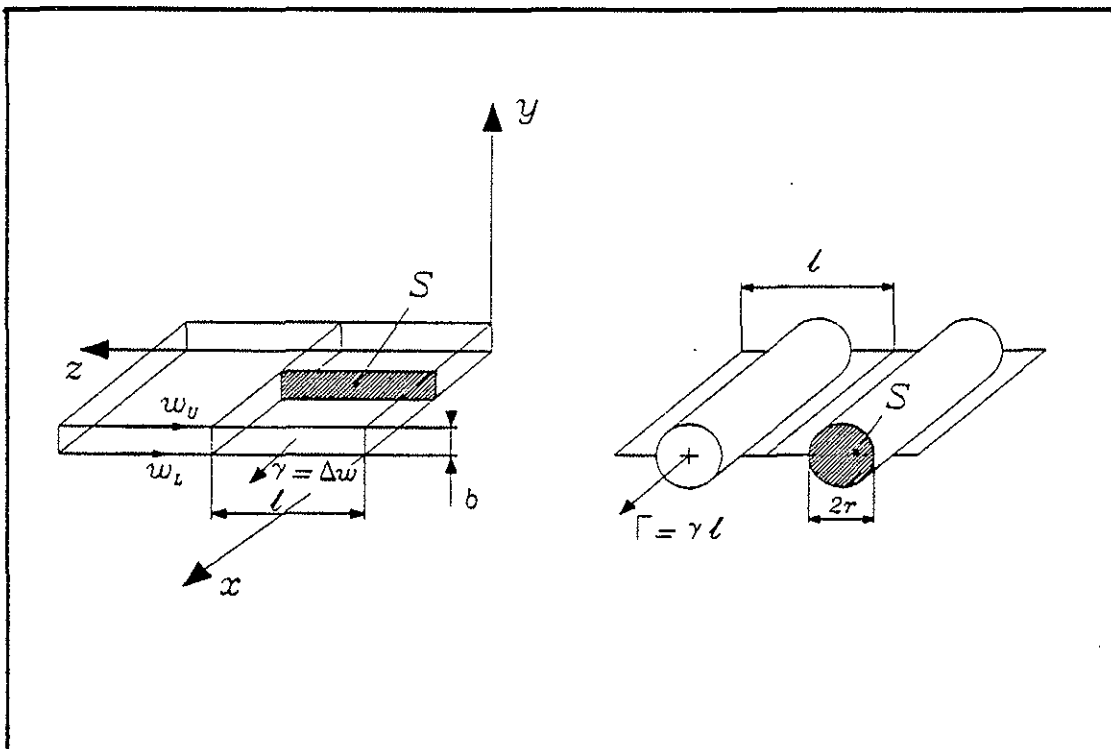


Fig.2 - Equivalence between elementary portions of a continuous shear layer and discrete Rankine vortices.

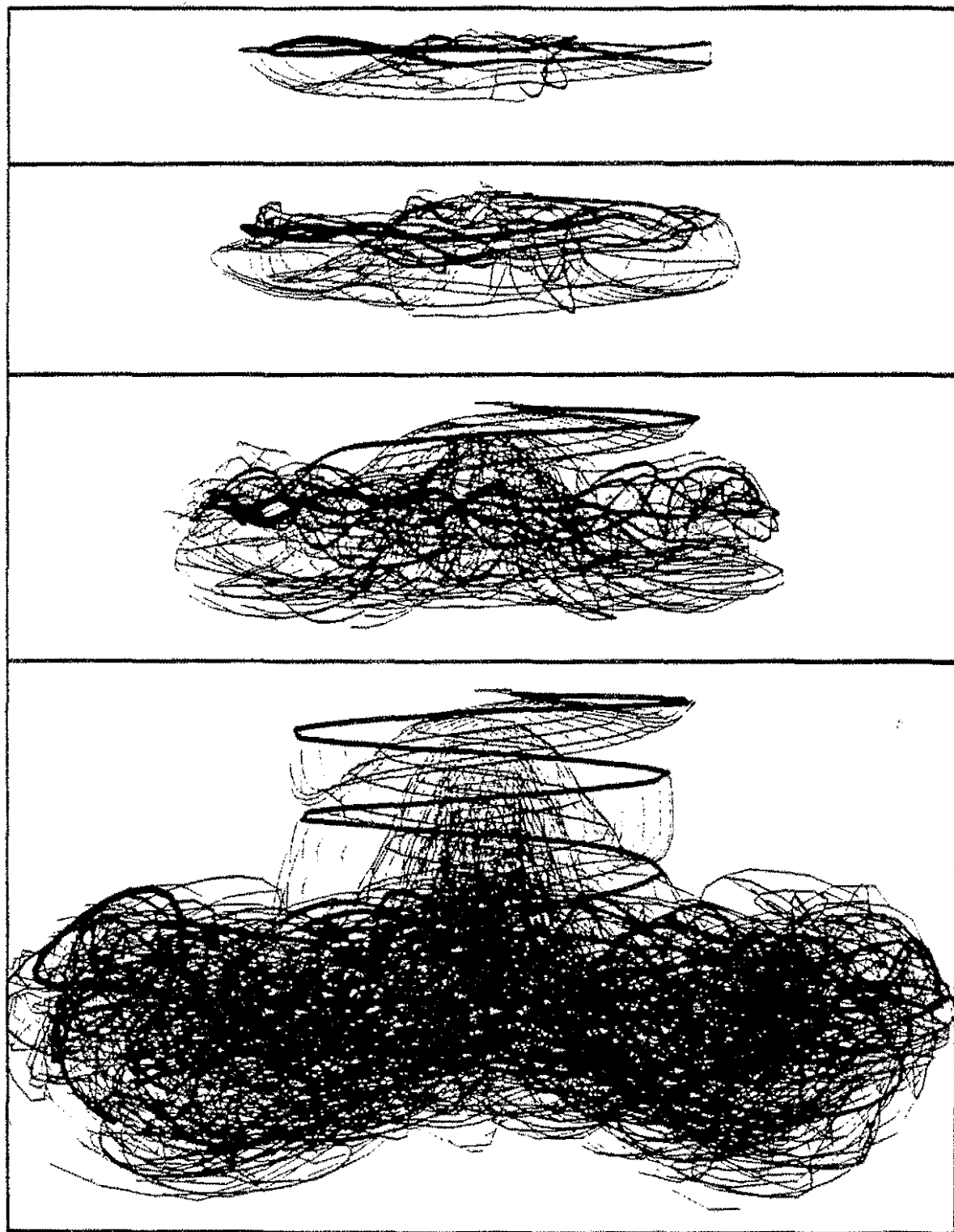


Fig.3 - Time evolution of the wake for an impulsively started two-bladed rotor in hover O.G.E. Lateral view of the wake of a single blade after 1, 2, 4, and 10 rotor revolutions. Line thickness proportional to vortex circulation.

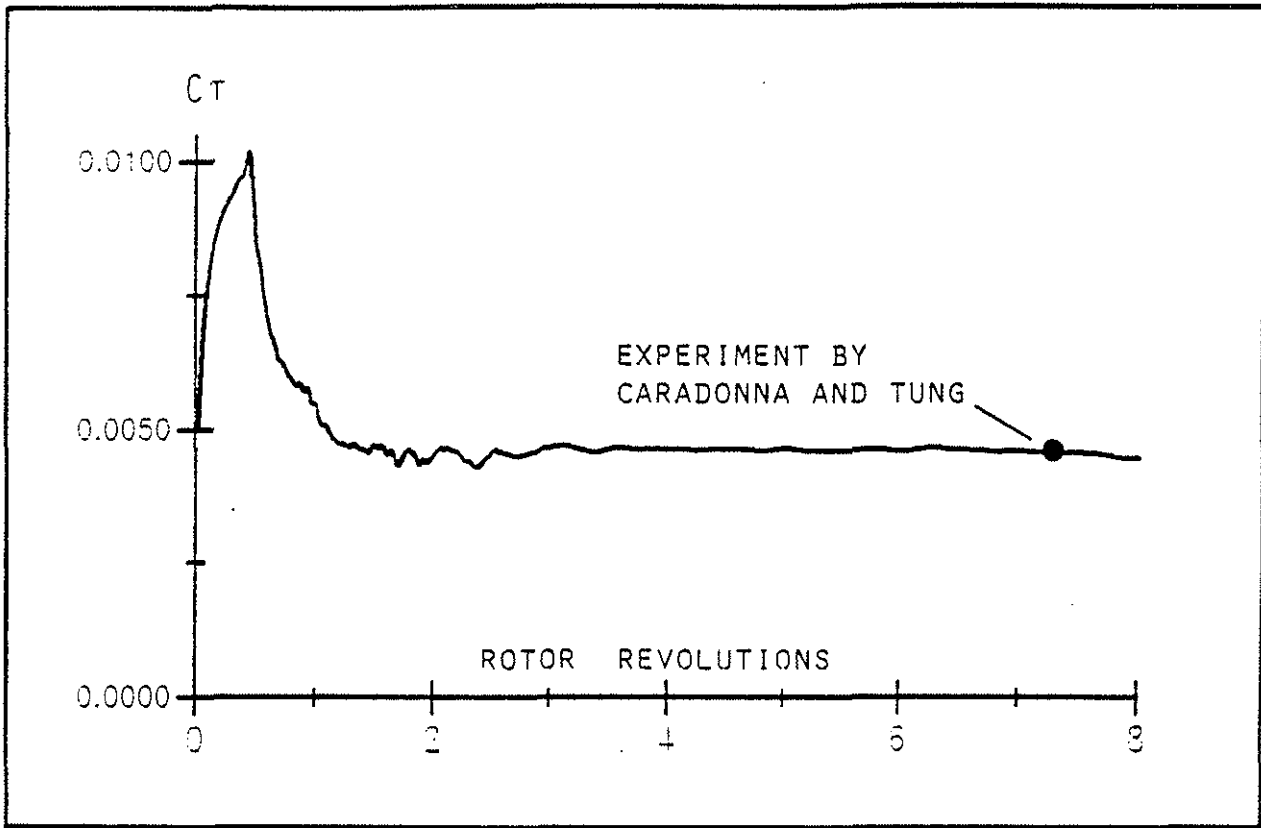


Fig.4 - Time evolution of thrust coefficient C_T for an impulsively started two-bladed rotor in hover O.G.E. Steady state measurement by Caradonna and Tung (1981).

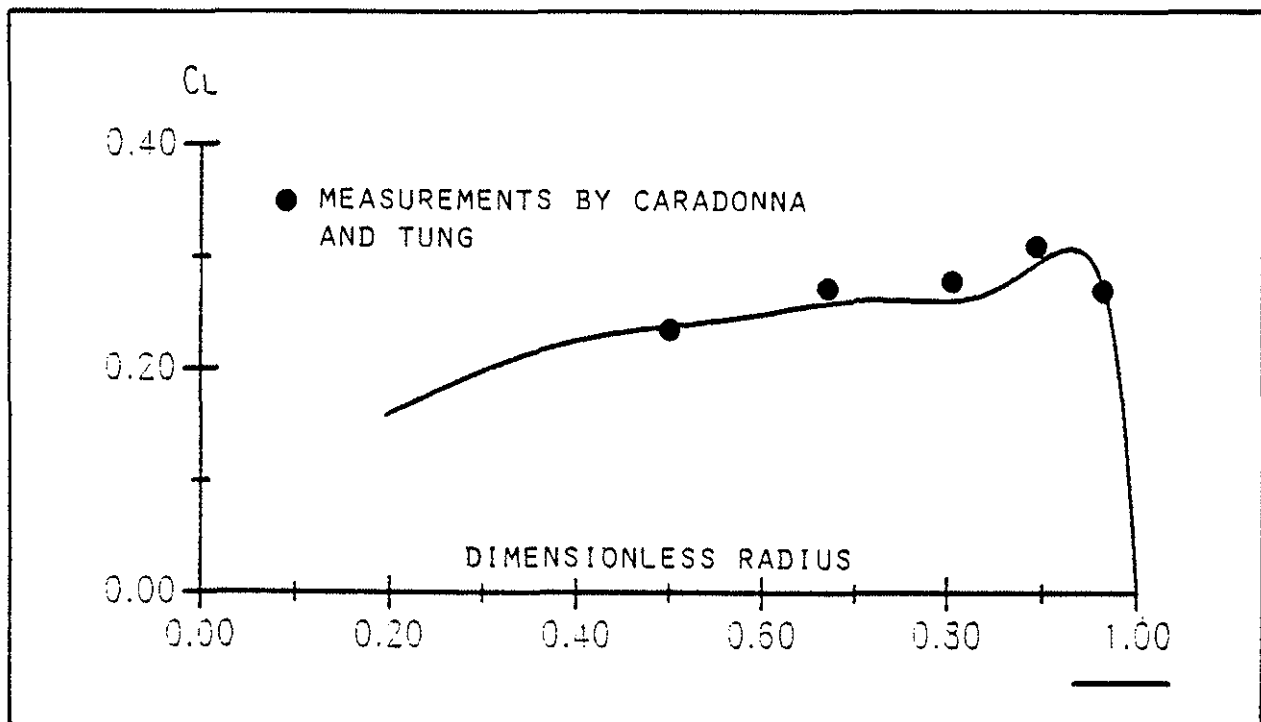


Fig.5 - Steady state radial distribution of local lift coefficient C_L for a two-bladed rotor in hover O.G.E. Steady state measurements by Caradonna and Tung (1981).

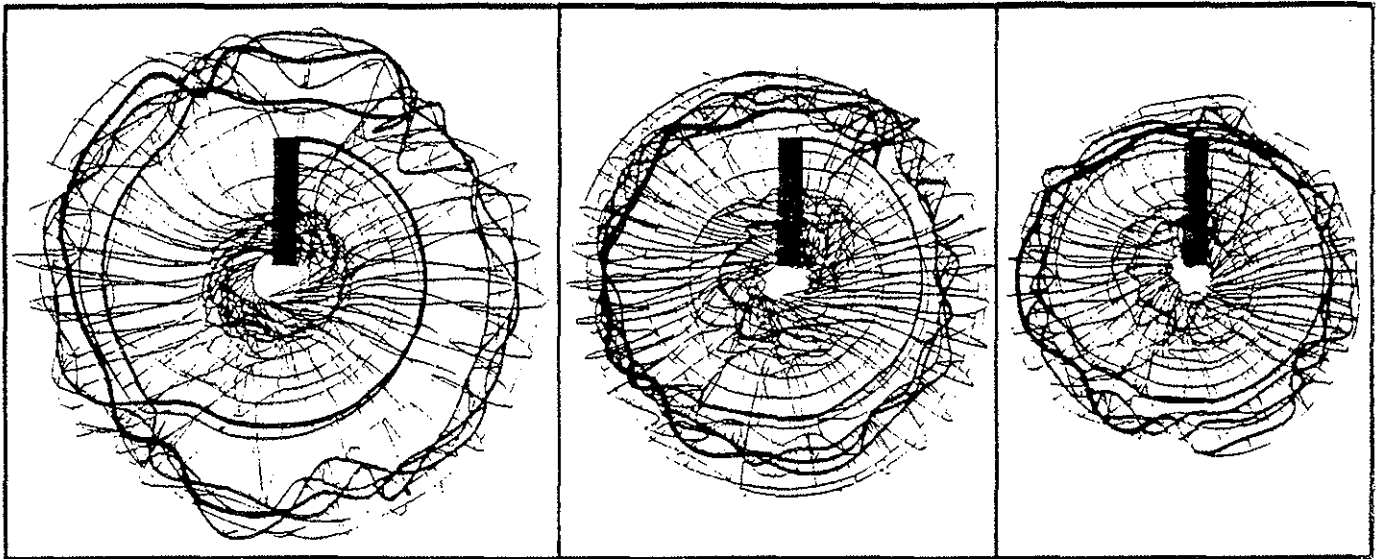


Fig.6 - Plan view of the wakes, after 3 rotor revolutions, for an impulsively started two-bladed rotor in hover I.G.E (rotor plane at 0.25 and 0.5 rotor tip radius R from ground) and O.G.E. Line thickness proportional to vortex circulation.

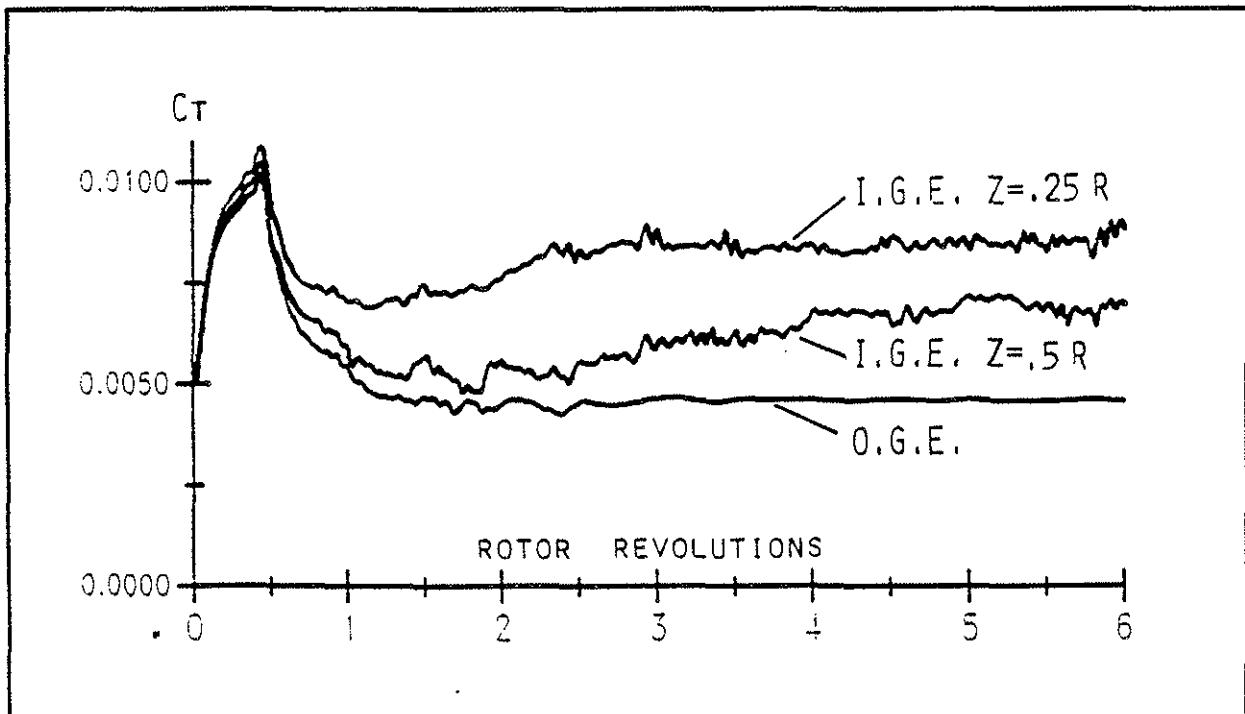


Fig.7 - Time evolution of thrust coefficient C_T for an impulsively started two-bladed rotor in hover I.G.E. (rotor plane at 0.5 and 1 rotor tip radius R from ground) and O.G.E.

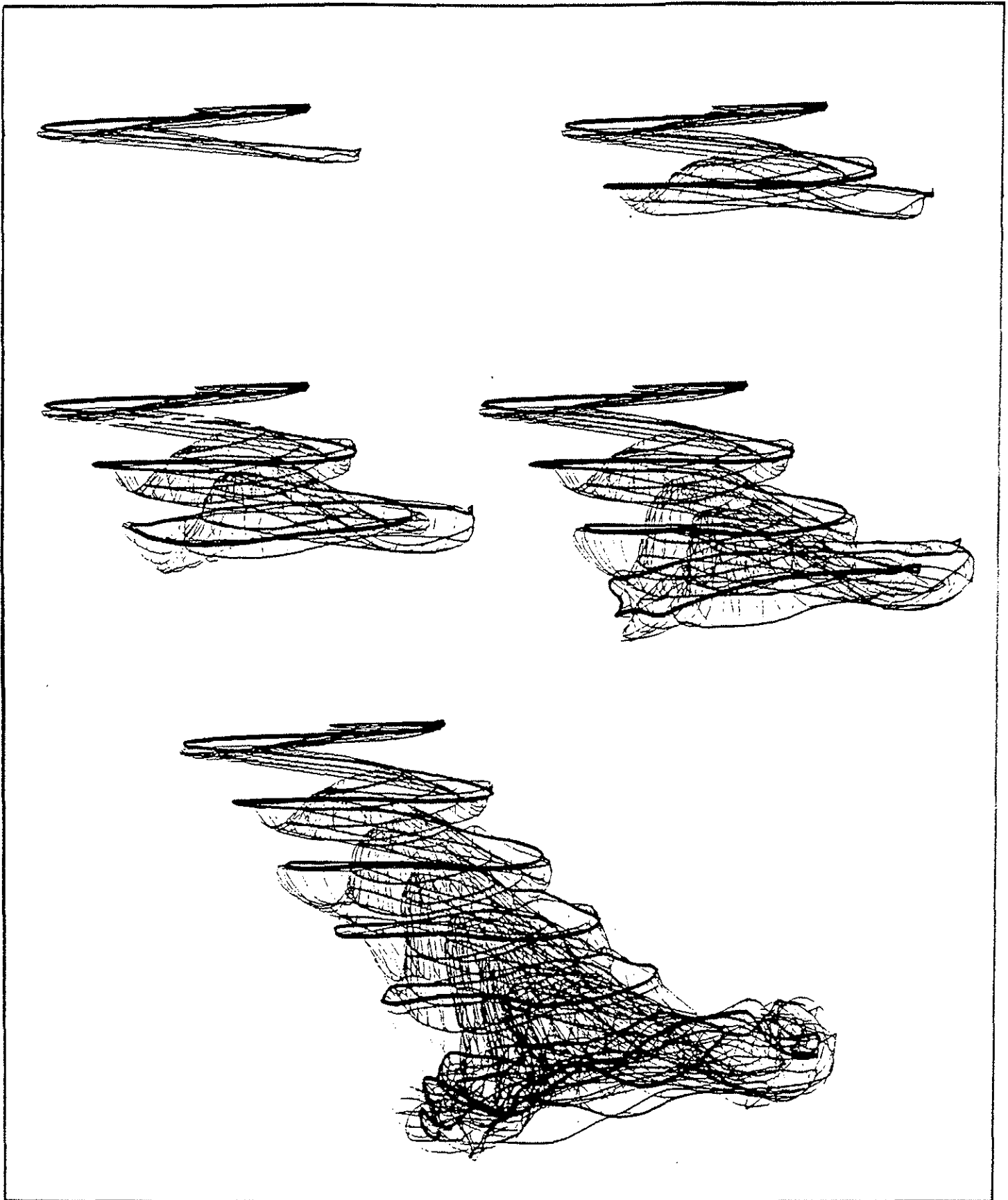


Fig.8 - Time evolution of the wake for an impulsively started two-bladed rotor in climbing forward flight ($\mu=0.05$, $\alpha=45^\circ$). Lateral view of the wake of a single blade after 1, 2, 3, 4 and 7 rotor revolutions. Line thickness proportional to vortex circulation.

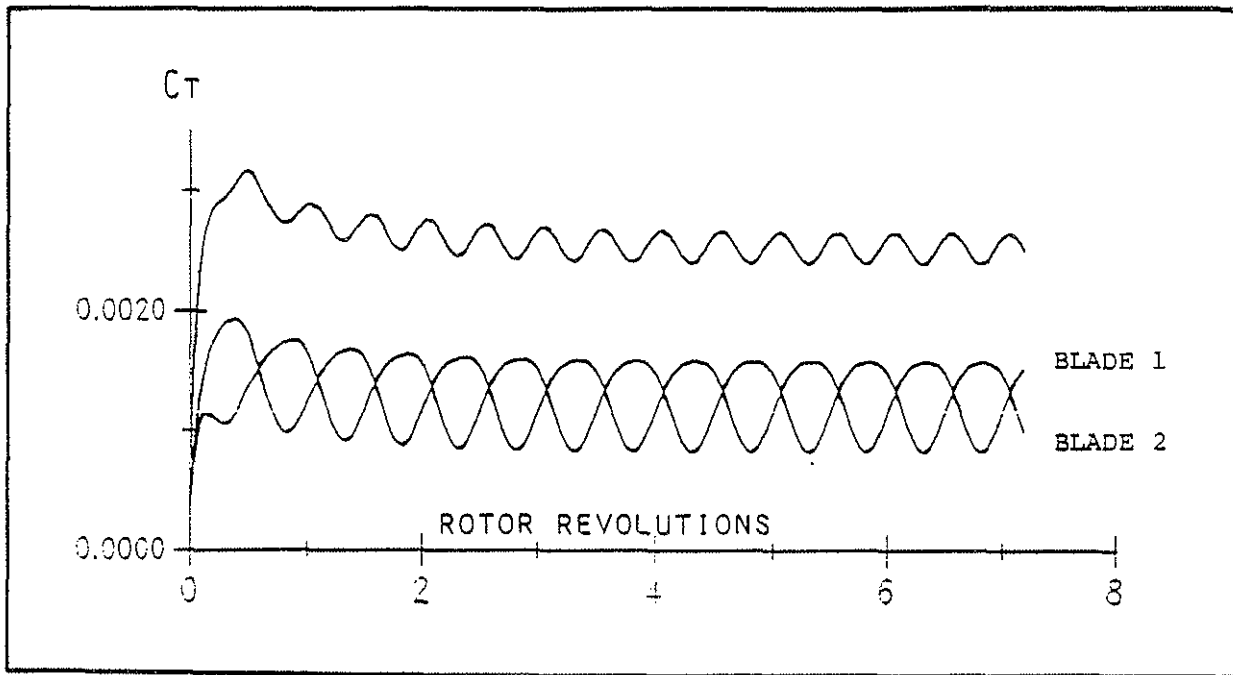


Fig.9 - Time evolution of thrust coefficient C_T for an impulsively started two-bladed rotor in climbing forward flight ($\mu=0.05$, $\alpha=45^\circ$).

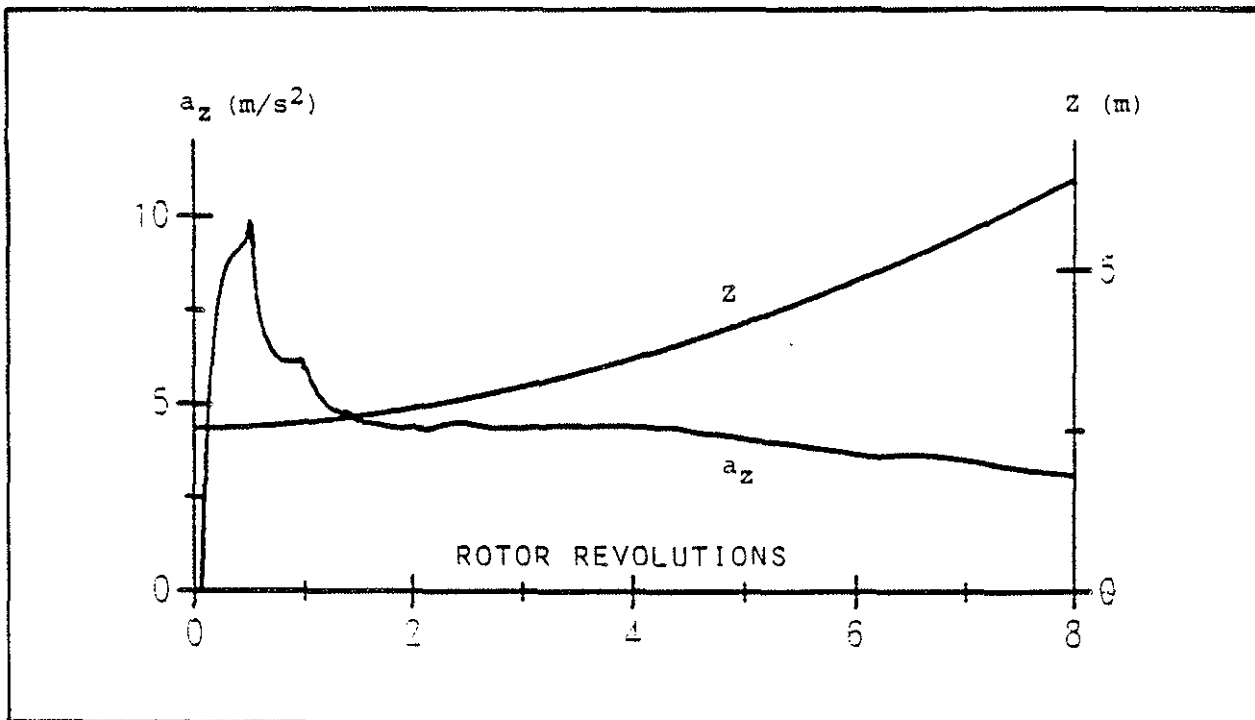


Fig.10 - Unsteady vertical take off I.G.E. Time evolution of helicopter vertical acceleration a_z and distance from ground z .

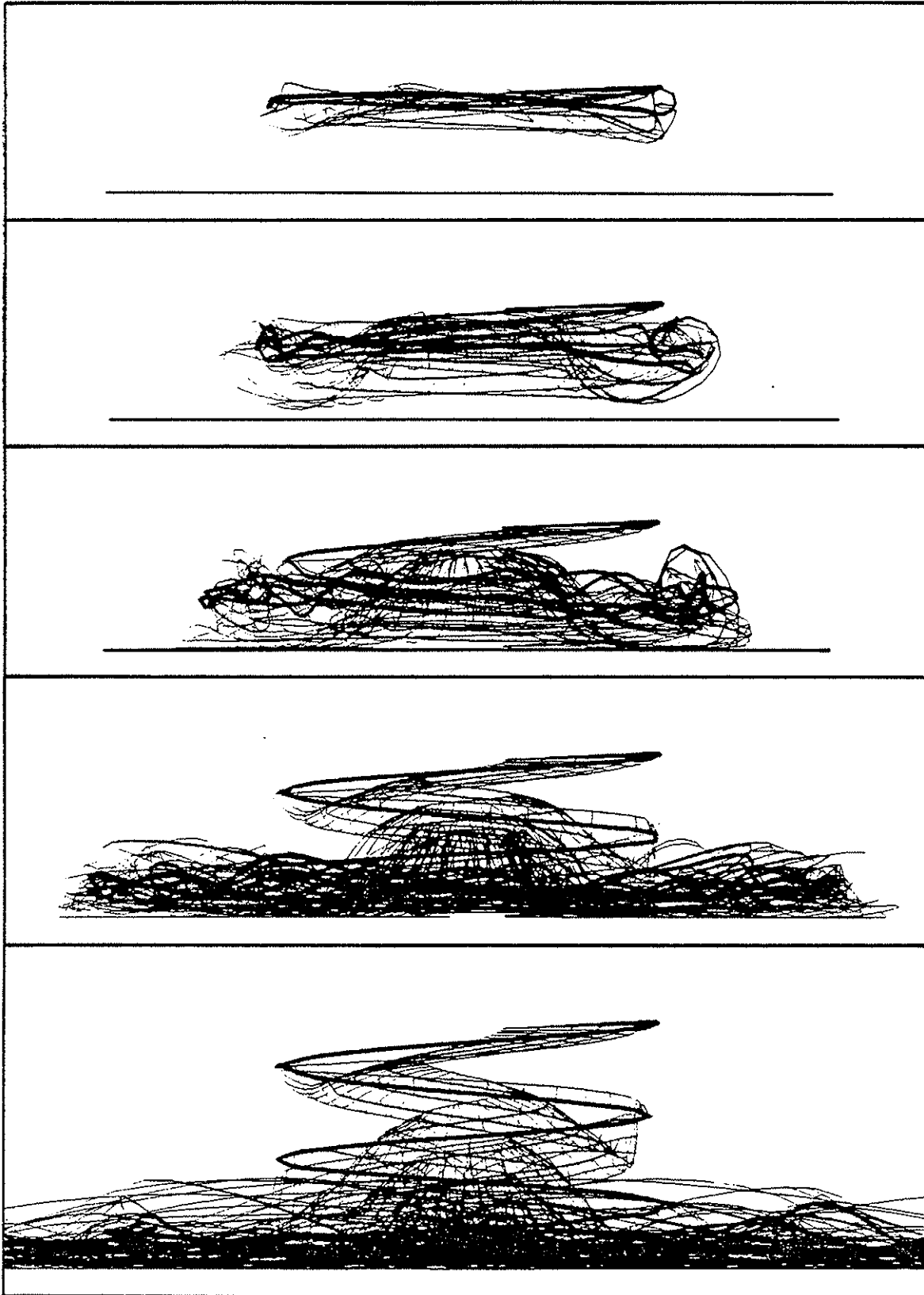


Fig.11 - Unsteady vertical take off I.G.E. Lateral view of the time evolution of the wake of a single blade, after 1, 2, 3, 5 and 8 rotor revolutions. Line thickness proportional to vortex circulation.